



# Phyllotaxis as a Dynamical Self Organizing Process

## Part I: The Spiral Modes Resulting from Time-Periodic Iterations

S. DOUADY AND Y. COUDER

*Laboratoire de Physique Statistique, 24 rue Lhomond, 75231 Paris Cedex 05, France*

*(Received on 12 January 1995, Accepted in revised form on 15 August 1995)*

This article is the first of a series of three in which the various phyllotactic modes are shown to result from successive iterations of two possible simple dynamical systems. In this first part the hypotheses put forward by Hofmeister (1868) for the formation of primordia are re-examined and shown to form the rules of such a system. By means of a physics experiment and a numerical simulation, it is demonstrated that this system gives rise to the self organization of the spiral phyllotactic structures. The dynamic is controlled by only one parameter,  $G$ , equivalent to Richards' plastochrone ratio (1951), which characterizes growth. The diagram representing the values of the divergence angle as a function of the plastochrone ratio resembles that obtained geometrically by van Iterson (1907). In the present results, however, only one branch of solutions is continuous for all values of  $G$ ; this difference with the geometrical results is important. The predominance of Fibonacci order in botany is related to this continuity: during the ontogeny, because of the continuous decrease in  $G$ , only this branch is followed. In this framework the build-up of such complex structures as the inflorescence of compositae is described.

© 1996 Academic Press Limited

### 1. Introduction

Phyllotactic patterns are generated whenever a vascular plant repeatedly produces similar botanical elements at its tip (leaves, bractae, florets etc). These patterns are surprisingly regular, so regular in fact that a physicist can compare their order to that of crystals. The observed organizations are classified in only two categories. In the first, formed of the distichous and spiral modes, the leaves appear one at a time along the stem. The striking peculiarity of this family is that it is directly related to the Fibonacci series and the golden mean. In the second, constituted of whorled modes, a constant number of leaves appear simultaneously at the same height on the stem and form successive whorls.

The investigation of phyllotactic patterns has a long history and was undertaken from several viewpoints. Recent reviews on this subject can be found in Williams (1975), Jean (1984, 1994) Steeves & Sussex (1989), Lyndon (1990), Sachs (1991) and Medford (1992). Three main lines of thought can be

recognized in the history of phyllotactic studies, each of them having brought major contributions to their understanding.

#### GEOMETRICAL APPROACH

The first investigations resulted from the direct observation of the arrangements of the elements on mature plants. Since the early works of Schimper (1830), Braun (1831, 1835), Bravais & Bravais (1837a, b, 1839), Airy (1873) and van Iterson (1907), the analysis of the geometry of the patterns has been aimed at a characterization of the observed spiral and whorled organizations of mature stems. More recent works in this domain were done by Erickson (1973), Rivier (1988) and Rothen & Koch (1989). This type of approach provided an analysis of the very specific properties of these dispositions. In particular, it was found that two different descriptions of the spiral order could be given. If the elements are linked in their order of appearance, the resulting curve forms a spiral (or a helix) called the generative spiral. Projected in the plane perpendicular to the stem, the

divergence angle  $\varphi$  between the base of two successive elements is constant and generally has a value close to  $\Phi = 2\pi(2 - \tau) = 137.5^\circ$ , where  $\tau$  is the golden mean  $\tau = (-1 + \sqrt{5})/2$ . In the second description, two sets of intersecting spirals are defined by linking each element to its nearest (or contact) neighbours. The numbers  $i$  and  $j$  of these spirals (the parastichies) around the stem are generally two successive terms of the main Fibonacci series: 1, 1, 2, 3, 5, 8, 13, 21, 34, . . . , in which each term is the sum of the two previous ones (the first two terms being 1 and 1). The Bravais brothers (1837a), showed that if the divergence angle  $\varphi$  was assumed to be equal to the ideal angle  $\Phi$ , the parastichies were then necessarily two consecutive Fibonacci numbers and that their particular values only depended on the longitudinal elongation of the stem. Airy (1873) was the first to consider the piling of elements of finite size instead of point like particles. In order to study the effect of a compression on a cylindrical piling he implemented an original system. He glued identical spheres onto an extended rubber band alternately on each side of the band (i.e. in a distichous disposition) and then slowly released the tension. As a result he observed transitions to the spiral modes (1, 2) and (2, 3). Inspired by this work, van Iterson (1907) systematically investigated the phyllotactic patterns obtained by paving a surface with solid elements, e.g. equal disks on a cylinder. He thus introduced a new parameter, the ratio  $b$  of the diameter of the disks over the perimeter of the cylinder. Without any other assumption he showed that, for a given value of  $b$ , spiral organizations were possible, corresponding to a series of well-defined values of  $\varphi$ . These values are a function of  $b$ , and the number of different possibilities increases with decreasing  $b$ , so that the graph  $\varphi(b)$  has the shape of a complex tree.

DYNAMICS OF GROWTH

A different approach was initiated when the apical region, where the formation of the primordia takes place, was observed using microscopic techniques. This led to consideration of the problem of how the phyllotactic structures appeared. Hofmeister (1868) was the first to systematically observe the apical region and to state general dynamical principles that, he suggested, led to the formation of the observed patterns. A smooth region of undifferentiated tissues, the apex is situated at the extremity of the shoot. Around it specific mitotic activity creates small protrusions, the primordia, which already form conspicuous parastichies and will evolve into various types of botanical elements: leaves, bracts, sepals, petals, stamens, florets etc. In the reference frame of

the apex, because the shoot grows with velocity  $U$ , the existing primordia drift away from the tip with a velocity  $V$  so that they leave room for the formation of new elements [Fig. 1(a)]. Hofmeister (1868) proposed that this inception is periodic in time and that the new primordium appears in the largest available space. The position of this primordium around the apex thus results from the position of the previous ones. Inspired by van Iterson's work, Snow & Snow (1952) tried to adapt Hofmeister's dynamical rules to the appearance of elements of a given finite size. Some of their experiments [Snow & Snow (1935)] also showed that there was a connection between the

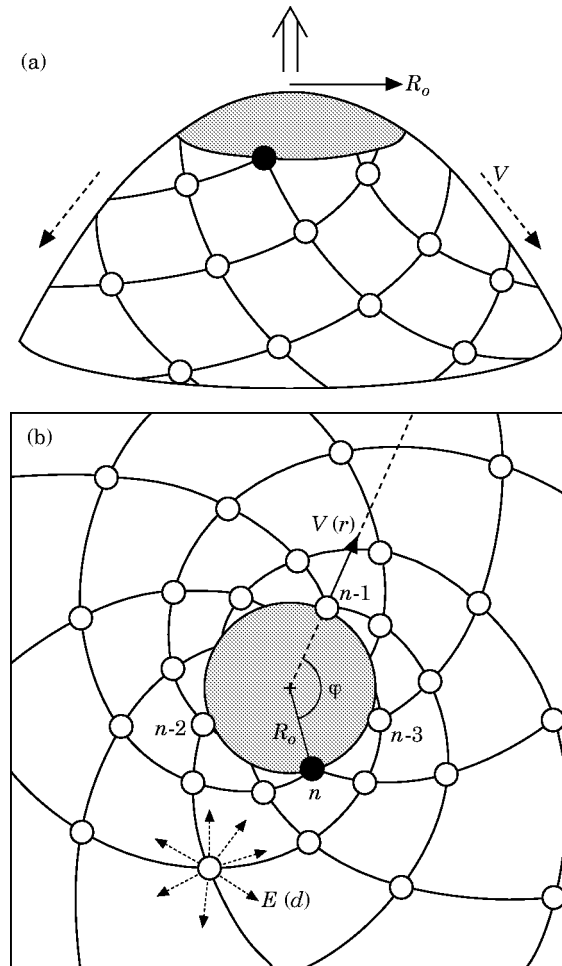


FIG. 1. Definition of the parameters of the apical growth. (a) Scheme of the botanical situation: given the growth of the shoot at velocity  $U$ , the resulting velocity at which the primordia move away from the tip is  $V$ . The incipient primordium is represented in black. It forms at the periphery of the apex of radius  $R_0$ , shown in grey. (b) The plane model of the apex. The position of the new primordium of appearance number  $n$  is defined relative to the previous one (of number  $n-1$ ) by the divergence angle  $\varphi$  and by the ratio of their distances to the centre:  $a = r_{n-1}/r_n$  (Richards' plastochrone ratio). The radial motion of each particle  $V(r)$  and the field lines of its repulsive potential  $E(d)$  are indicated.

whorled phyllotactic modes and the spiral ones. They thus suggested (Snow & Snow, 1962) removing the imposed periodicity of the process: a new primordium simply forms where and when there is enough space for its formation.

An important step in relating quantitatively the dynamics of the growth to the geometry of the resulting spirals was taken by Richards (1951) who introduced the plastochrone ratio  $a$ , a parameter of fundamental importance to quantify the growth and which will be described below.

Finally a completely different set of hypotheses was put forward by Plantefol (1948), in which he gave a specific role to one of the set of parastichies that he called foliar helices. These hypotheses, however, did not deal with the fact that the number of parastichies follow the Fibonacci series; they cannot, therefore, be used here. In fact, as we will see, they do not seem to be compatible with the minimal hypotheses necessary to get this type of ordering (see Section 5).

#### PHYSIOLOGY OF THE APICAL MERISTEM

A third direction for research was aimed at the determination of the physiological processes responsible for the interaction between the primordia. Several models were put forward in which the interaction was ascribed to the contact pressure (Schwendener, 1878; Airy, 1873; van Iterson, 1907; Church, 1904; Adler, 1974; Williams & Brittain, 1984), to the diffusion of an inhibitor (Schoute, 1913; Wardlaw, 1968; Mitchison, 1977), to a reaction-diffusion process (Turing, 1952; Meinhardt, 1974; Veen & Lindenmayer, 1977; Young, 1978; Chapman and Perry, 1987) or to a buckling instability due to a differential growth of the apical surface (Green, 1992). All these types of interaction create either a repulsion or an inhibition between primordia so that the incipient primordium will form as far away as possible from the previous ones and thus in the largest available space. They are, therefore, compatible with the dynamical principles defined both by Hofmeister (1868) and by Snow & Snow (1952).

These three main points of view are complementary and a complete understanding of the phyllotactic processes will require a synthesis of results obtained along these three directions of research. The link between these different approaches is obvious: the geometry of the patterns results from a dynamic of formation and this dynamic is created by interactions caused by physiological processes. The actual physiological process involved is not yet identified with certainty, but most of those that have been suggested result in similar types of interactions. It is thus possible, and justified, to examine the resulting

dynamics *per se*. This is our limited aim: we are concerned here with the minimal dynamical hypotheses necessary to give rise to the phyllotactic patterns. In this first article we thus return to the hypotheses of Hofmeister (1868) and in the second and third (Douady & Couder, 1996a, b) we will revisit those put forward by Snow & Snow (1952). It must be kept in mind, however, that even if we are successful in realistically reproducing the build-up of the phyllotactic patterns, the underlying physiological processes will still have to be identified.

## 2. The First Iterative Model

The remarkable feature of the dynamical hypotheses is that they do not have any specific effect directly caused by the biological nature of the system. Rather, they define the principles of an iterative system, in which the repeated application of the same rule gives rise to the successive states. Our aim was to see whether these principles were able, by themselves, to produce the spiral organizations hitherto only observed in plants. We thus tried to find a non-biological system reproducing the dynamical characteristics given by Hofmeister's hypotheses [preliminary results can be found in Douady & Couder (1992, 1993)]. In order to implement both a laboratory experiment and a numerical simulation, we used a simplified model of the apical meristem [Fig. 1(b)] and retained the following characteristics:

First set of Hypotheses (Hofmeister, 1868)

- The stem apex is axisymmetric.
- The primordia are formed at the periphery of the apex and, due to the shoot's growth, they move away from the centre with a radial velocity  $V(r)$ .
- New primordia are formed at regular time intervals (the plastochrone  $T$ ).
- The incipient primordium forms in the largest available space left by the previous ones.
- Outside of a region of radius  $R_0$  there is no further reorganization leading to changes of the angular positions of the primordia.

In the first series of experiments and numerical simulations we will limit ourselves to situations where the apical meristem is planar and the primordia have circular symmetry. The fact that the same phyllotactic arrangements are observed for different transverse profiles of the apical meristem suggests that its conicity is not a parameter of prime importance (this statement will be re-examined in Part II (Douady & Couder, 1996a)). In order for the new element to appear in the largest available space, we assume that

it is submitted to repulsive forces generated by the previous elements. This is just the simplest physical implementation of this rule, but it does not mean that there is necessarily a physical force between the primordia: an inhibitory interaction would have an equivalent effect, and so would the interaction of the successive bulges of a buckling instability. In the numerical simulations, this can even be considered as a simple way to easily find the largest space.

In botanical reality the primordia do not change angular position after their formation, and their later motion is purely radial. This condition is important in order to obtain phyllotactic patterns. If long-term reorganizations were allowed, the lattice of repelling elements would tend to form a hexagonal pattern with some dislocations. We will see that in the experiment this absence of late interactions does not have to be imposed: the radial motion is sufficient to lead the elements apart from each other so that their interaction vanishes. Finally, in botanical reality, the growth near the apex is exponential so that the velocity  $V(r)$  is proportional to  $r$ .

### 3. The Experiment

#### 3.1. SET UP

The experimental set up [described in more detail elsewhere (Douady & Couder, 1992, 1993)] consists of a horizontal teflon dish of diameter 8 cm filled with silicone oil, placed in a vertical magnetic field (Fig. 2). This field  $\mathbf{H}(r)$  has a weak radial gradient: it is minimal at the centre and maximal at the periphery. The primordia are simulated by drops of ferrofluids. These are liquid suspensions of magnetic particles and have the properties of a ferromagnetic fluid. A drop

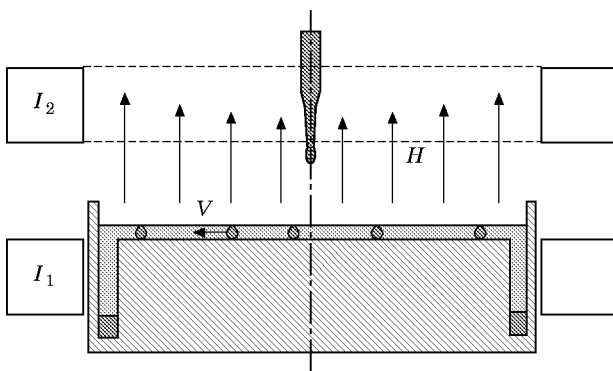


FIG. 2. Sketch of the experimental apparatus. Drops of ferrofluid are used to simulate the primordia. The drops (of volume  $v \approx 10 \text{ mm}^3$ ) fall with a tunable periodicity  $T$  at the centre of a horizontal teflon dish. The vertical magnetic field  $H$  is created by two coils in the Helmholtz position. The dipoles are radially advected with velocity  $V$  by the magnetic field gradient (controlled by the currents  $I_1$  and  $I_2$  in the two coils). The drops ultimately fall into a deep ditch at the periphery, designed to prevent accumulation.

of ferrofluid placed in a magnetic field is polarized and forms a small dipole with its moment parallel to the field. In the present experiment, a drop deposited at the centre of the dish forms a dipole with a vertical moment which is attracted towards the region of maximum field. The drop thus spontaneously drifts from the centre to the border of the dish with a velocity  $V(r)$  limited by the viscous friction of the oil. Drops of equal volume ( $v \approx 10 \text{ mm}^3$ ) can be deposited with a tunable periodicity  $T$  at the centre of the cell. As these drops form identical parallel dipoles they repel each other with a force proportional to  $d^{-4}$  ( $d$  being their distance).

In this system the radial motion of the drops replaces growth, and their periodic introduction simulates the periodicity of the primordium formation. Furthermore, the repulsion caused by the previous drops forces the new one to place itself in the largest available space at the periphery of the central region. We have thus realized a system where all but one of the necessary characteristics have been reproduced. The only problem is that, in order to avoid breaking the symmetry of this experimental system, it is necessary to introduce the elements at the centre instead of at the periphery of a circle. For this reason the bottom of the cell was built with a small central bump which makes this position unstable for the new drop: it thus moves swiftly away from the centre. Moving down from this bump, the new drop falls in the direction resulting from the repulsion of the previously deposited drops.

The experiment is observed from above with a videotape camera. The recordings show the pattern formed by the drops as well as the trajectory of each drop. A superposition of video tape images taken at different times shows that in a central region of radius  $R_c$ , some organization of the pattern takes place, but that outside this region ( $r > R_c$ ) the drops have only a radial motion as they have moved too far away from each other to interact.

#### 3.2. RESULTS

In practice the experimental control parameter is the periodicity of the fall of the drops. For a given value, after a short, transient period, steady regimes are reached and the positions of the successive drops form reproducible patterns. For large values of  $T$  [Fig. 3(a)] a given drop, after its fall, is repelled only by the previous drop because, all the others having moved far away, their repulsion is negligible. Each drop moves away in the direction opposite to the previous one. The divergence angle is thus  $\varphi = 180^\circ$  and the pattern corresponds to the distichous mode which is common in botany. If the periodicity  $T$  is

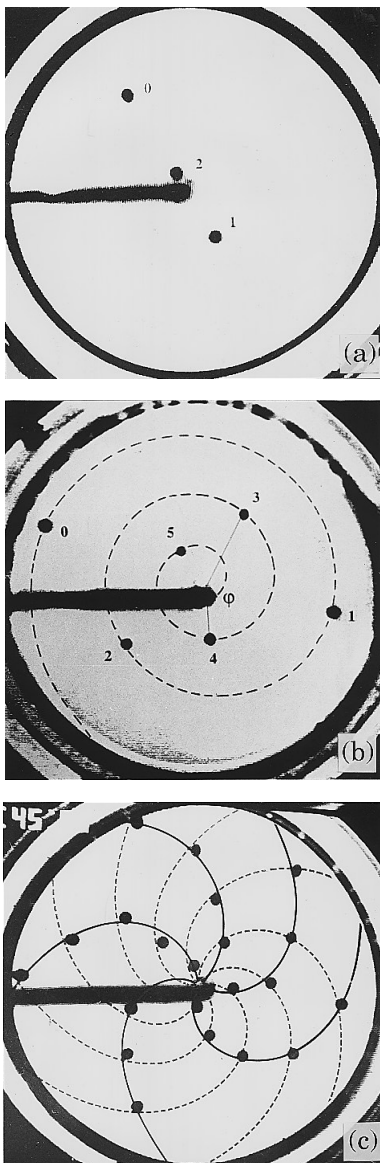


FIG. 3. Three photographs (seen from above) of typical phyllotactic patterns formed by the ferrofluid drops for different values of the control parameter  $G$ . The drops are visible as dark dots. The tube for the ferrofluid supply partially hides the central truncated cone. The drops are numbered in their order of formation. (a) For strong advection,  $G \approx 1$ , each new drop is repelled only by the previous one and a distichous mode is obtained,  $\varphi = 180^\circ$ . (b) Below the first symmetry breaking bifurcation ( $G \approx 0.7$ ) the successive drops move away from each other with a divergence angle  $\varphi = 150^\circ$  (shown between drop three and four). They define an anti-clockwise generative spiral (dashed line). The parastichy numbers correspond to (1, 2). (c) For smaller advection ( $G \approx 0.1$ ) higher order Fibonacci modes are obtained. Here  $\varphi \approx 139^\circ$  and the parastichy numbers are (5, 8).

decreased, a remarkable evolution of these patterns takes place. Below a threshold value each new drop becomes sensitive to the repulsion of the two previous drops and can no longer remain on the radial line formed by them. In such a case the third deposited drop slides to one of either side of the line formed by

the first two (see also Figs 6 and 7). This is a symmetry breaking bifurcation which selects once for all the direction of winding of the generative spiral. A steady regime is reached later with a constant divergence  $\varphi$  [in Fig. 3(b)  $\varphi = 150^\circ$  and two parastichies  $i=1, j=2$  are observed]. For smaller  $T$ , the new drop becomes sensitive to the repulsion of three or more previous drops, and the divergence gets nearer to  $\Phi$ . In Fig. 3(c),  $\varphi = 139^\circ$  and the Fibonacci numbers are  $i=5, j=8$ . The spiral mode obtained in this non-biological system is strikingly similar to a very usual organization observed in botany.

### 3.3. DISCUSSION

The observed patterns, in fact, do not depend only on  $T$ , but also on  $R_c$  the radius of the circle outside of which the angular position of the particles is fixed, and on the advection velocity  $V_o$  (controlled by the magnetic field gradient). The only relevant parameter is in fact adimensional and defined by  $G = V_o T / R_c$ . It is the ratio of the two typical length scales of the system, one corresponding to the radial displacement of the elements during one period and the other defining the size of the central region. This parameter is directly related to the plastochrone ratio,  $a$ , which was introduced by Richards (1951). This author showed that the apical growth could be characterized by the ratio  $a = r_{n-1} / r_n$  of the distance of two successive primordia to the centre. This ratio is easily measured on transverse sections of apices. The relation between  $a$  and  $G$  is simple because the growth near the apical region is exponential. As  $V(r) \propto r$  and  $V(R_o) = V_o$ , the distance of a primordium to the centre at time  $t$  is:  $r = R_o \exp(V_o t / R_o)$  and its velocity  $V = V_o \exp(V_o t / R_o)$ . The resulting plastochrone ratio is  $a = r_{n-1} / r_n = \exp(V_o T / R_o)$  and our parameter  $G$  is simply:  $G = \text{Ln}(a)$ . This parameter had been used previously in botanical cases by Meicenheimer (1979) and by Rutishauser (1982).

The only precise way of measuring  $G$  both in plant growth and in our experiment is to deduce it from  $a = r_{n+1} / r_n$ . In plants, obtaining  $G$  from measurements of  $V_o$ ,  $T$  and  $R_o$  would be more difficult and less precise than deducing it from the geometry of transverse sections. In our experiment  $V_o$  and  $T$  are known with precision, but there is ambiguity on the choice of  $R_o$  because the drops are introduced at the centre of the cell. If we deduce a value of  $R_o$  from the measured plastochrone ratio we find that, in all cases,  $R_o$  is equal to  $R_c$  the radius of the circular zone out of which there is no further reorganization and change of  $\varphi$ . This result could have a meaning in botany. It is well known that the angular positions of the primordia become rapidly fixed at the apex

periphery and do not change during the later growth of the stem. This does not, however, preclude slight changes of  $\varphi$  at a very early stage by asymmetrical growth of a primordium. There has also been some discussion about when exactly (i.e. at which radius) the growth of primordia starts, and where its position becomes fixed. From the dynamical point of view the only relevant length scale is the radius  $R_c$  such that for  $r > R_c$  there is no change of  $\varphi$ . Our experiment shows that this is the length deduced from the measurements of the plastochrone ratio. If the botanists could measure both  $V$  and  $T$ , the radius  $R_c$  could be directly derived from the plastochrone ratio. It would then be interesting to compare it to the apparent apex radius.

The values of  $G$  obtained in the experiment range from 1 [Fig. 3(a)] to 0.1 [Fig. 3(c)]. We can note that in our laboratory experiment a value of  $G=1$  is obtained with  $V_o \approx 1 \text{ cm s}^{-1}$ ,  $T \approx 1 \text{ s}$  and  $R_o \approx 1 \text{ cm}$ . In botany,  $R_o$  and  $T$  can be measured directly and  $V_o$  can then be deduced from measurements of the plastochrone ratio of the type done by Schwabe (1971), Williams (1975) and Erickson & Meichenheimer (1977). Revisiting their data, the orders of magnitude of each of these variables can be estimated. They are completely different from those of the laboratory experiment but they result in similar values of the adimensional combination  $G$ . For instance  $G=1$  can be reached in plants with such typical values as  $V_o \approx 10^{-3} \mu\text{m s}^{-1}$ ,  $T \approx 10^5 \text{ s}$  and  $R_o \approx 100 \mu\text{m}$ . This is the reason for which, even though our experiment appears so different from the botanical situation, the same organizations can be obtained. We will present our results as a function of  $G$ . It can be noted that they could also be conveniently plotted as a function of  $\text{Ln}(G)$  which is  $\text{Ln}[\text{Ln}(a)]$  [Richards, 1951, actually used  $\log_{10}(G)$ ]. With this latter variable the domains of existence of the successive phyllotactic modes would be approximately equal. This corresponds to the observation of van Iterson (1907) and Richards (1951), which led the latter to introduce a plastochrone index  $P.I. = 0.379 - 2.3925 \log_{10}[\log_{10}(a)]$ . The integer nearest to the value of this index gives the order of the parastichy system. We will not use this system as it is only an approximation relying on the assumption that the divergence angle  $\varphi$  is exactly equal to  $\Phi$ .

## 4. The Simulation

### 4.1. PRINCIPLE

The simulation permits a further simplification and thus corresponds more strictly than the experiment to minimal hypotheses. Like the experiment, it is

performed in a plane radial configuration. The locus of appearance of the elements is a circle  $C$  of radius  $R_o$  centred at the origin. The elements are point-like particles, each generating a repulsive energy  $E(d)$  where  $d$  is the distance to the particle. To be compatible with botanical observations, all the elements, after their formation are given the same radial motion with a velocity  $V(r)$ . We thus do not allow any possible reorganization by later interactions between the particles. The repulsive energy can be considered here as being simply a way to compute the largest space left by the other particles: its only consequence is the decision of where the new element will be placed. The whole organization thus occurs only on the circle when a new element is formed.

The most important possibility opened by the numerical simulation is the choice of the criterion for the appearance of a new particle.

We can simulate the Hofmeister principles (and thus the experiment) by imposing a temporal periodicity  $T$  to the formation of a new element. In order to decide the place of appearance of the incipient particle at each period  $T$ , we compute the value of the total energy caused by the previous particles along the circle  $C$ . The new element is placed at the point of the circle where this energy is at its minimum, corresponding to the largest possible space. It can be noted that the potential at this minimum does not have a fixed value, so that the size of the available space around it is not fixed either.

We can also simulate the iteration principles deduced from the Snows' hypothesis, something impossible to implement in our experiment. In this latter case, to be presented in Parts II and III (Douady and Couder, 1996a, b), the time of formation of the elements will be left free but the potential at which the formation occurs will be fixed.

It is also possible in the simulation to investigate the effect of different velocity laws: most simulations were done with  $V(r)$  increasing linearly with  $r$  [i.e.  $V(r) = V_o r / R_o$ ], a dependence which corresponds to the exponential growth observed in plants near the apical meristem. Other  $V(r)$  dependences, however, were explored [ $V(r) = V_o$  or  $V(r) = V_o R_o / r$ ]: the results are qualitatively the same. Different types of energy laws  $E(d)$  were also used, such as  $1/d$ ,  $1/d^3$  (which is the interaction between the ferrofluid drops), and  $\exp(-d/l)$ : again we found qualitatively the same results.

Finally, we can also explore the role of initial conditions and the transient regimes. Before the beginning of the iterations we can place a certain number of initial particles in chosen positions. In this

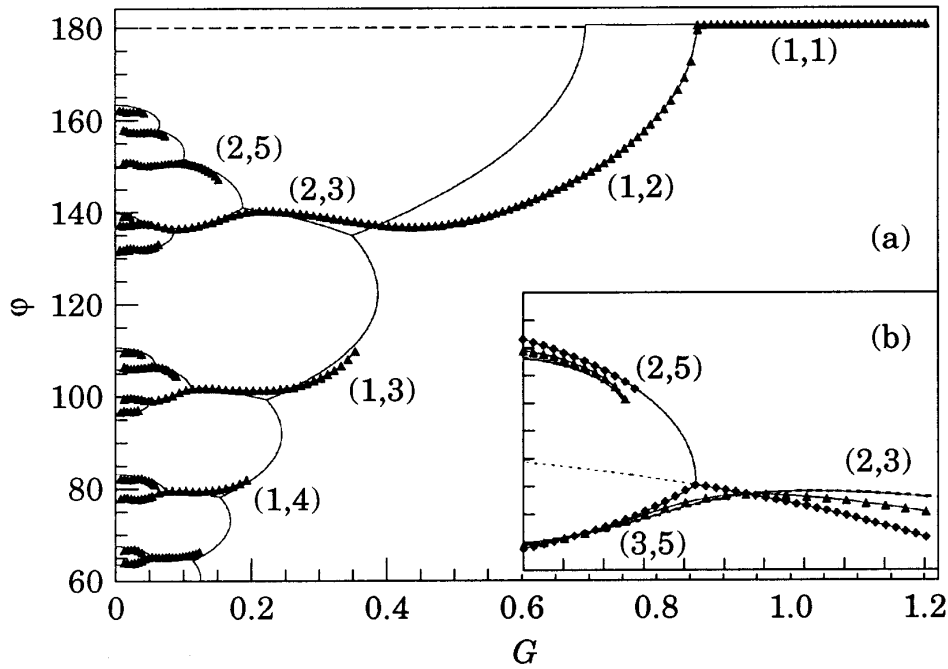


FIG. 4. The possible steady regimes obtained in the numerical simulation. (a) Diagram of the values of the steady divergences  $\varphi$  obtained in the simulation as a function of  $G$  (triangles). Each point represents a value of the divergence obtained in the simulation when the system has reached a steady regime. For some of the values of  $G$  this sometimes required up to 400 iterations. The velocity corresponds to an exponential growth and the energy profile is  $E(d)=1/d^3$ . The thin lines are the results of the geometric approximation where the new particle is assumed to appear exactly equidistant from two older ones. They form a diagram similar to that obtained by van Iterson. (b) Detail of a bifurcation showing the effect of a change in the interaction law (—)  $E(d)=1/d$ , ( $\Delta$ )  $E(d)=1/d^4$ , ( $\bullet$ )  $E(d)=\exp[-d/l]$  with  $l=0.01$ . Continuous line: geometric approximation.

way, we can reach all the stable modes of the iterative system.

The numerical simulations were done on Macintosh computers MIIIfx, Quadra 950 and Quadra 840 av. The programme was written in Think Pascal (18 pages, mostly used for the presentation). The only task is to find the minimum of the repulsive potential caused by all the previous elements at the imposed time. To do so, we first compute the potential on a discrete set of points on the circle. The point where the potential is minimum is then picked up, and again a discrete set of points around it taken. We then repeat this procedure several times until the required precision (typically  $0.1^\circ$ ) is reached. To be sure that the first point chosen is close to the absolute minimum, it is sufficient to take an initial number of points 20 times larger than the number of primordia which are close to the apex boundary [typically  $i+j$  for an  $(i, j)$  spiral pattern].

The potential is computed by adding up the contributions of a limited number of previous elements. This number is chosen so that the result does not change if a larger number is taken. It depends on the pattern, and on the chosen potential.

Typically two or three times  $(i+j)$  are more than enough for an  $(i, j)$  spiral pattern. We add up the contributions of the elements by inverse order of appearance, from the youngest to the oldest. To speed up the search for the point closest to the minimum potential, we keep in memory the smallest potential already computed for the previous iteration. The summation is stopped as soon as the value obtained is larger than the recorded minimum. After an optimization of the programme, typically one minute is enough to compute two hundred iterations.

4.2. RESULTS

The first result is that the simulation, like the experiment, mostly leads to steady regimes. For each given value of the parameter  $G$  there exists one or several situations for which each element is formed at a constant divergence angle  $\varphi$  from the previous one. When there are several possible regimes with different values of  $\varphi$  for the same value of  $G$ , the one which actually appears depends on the initial conditions, or on the transient which has led to this value of  $G$ . We will see that the ontogeny of the plant imposes specific

transients and thus a selection from these possible solutions.

In order to explain the spiral structures observed in botany we will first examine all the possible permanent states of the simulation and then return to the botanically relevant transients resulting from continuous time variations of  $G(t)$  during ontogeny.

*The permanent regimes*

The simulation permits very long iterations (e.g. the successive formation of 400 particles) so that steady regimes are reached. We represent these states in a  $\varphi(G)$  diagram [Fig. 4(a)]. For large values of  $G$  the position of each particle is determined by the repulsion of the previous one so that the distichous mode with  $\varphi = 180^\circ$  is observed. As in the experiment,

at a well-defined threshold value  $G_c$ , the alternate mode, ceases to be stable. Below this value two spiral modes become possible with  $\varphi < 180^\circ$  and  $\varphi > 180^\circ$ , respectively, corresponding to the two opposite directions of winding. Near the threshold of this first bifurcation, the divergence  $\varphi$  varies as  $|180^\circ - \varphi| \propto (G_c - G)^{1/2}$ , and the number of iterations (i.e. of particles) necessary to reach a steady regime diverges. These are the characteristics of what is called, in the dynamical systems terminology, a symmetry breaking bifurcation. In the present case the system acquires chirality as it goes from an alternate pattern to a clockwise or anti-clockwise spiral pattern. From now on we will only describe the modes with one direction of winding (Fig. 4). It must be kept in mind that each of them has a symmetric with opposite chirality.

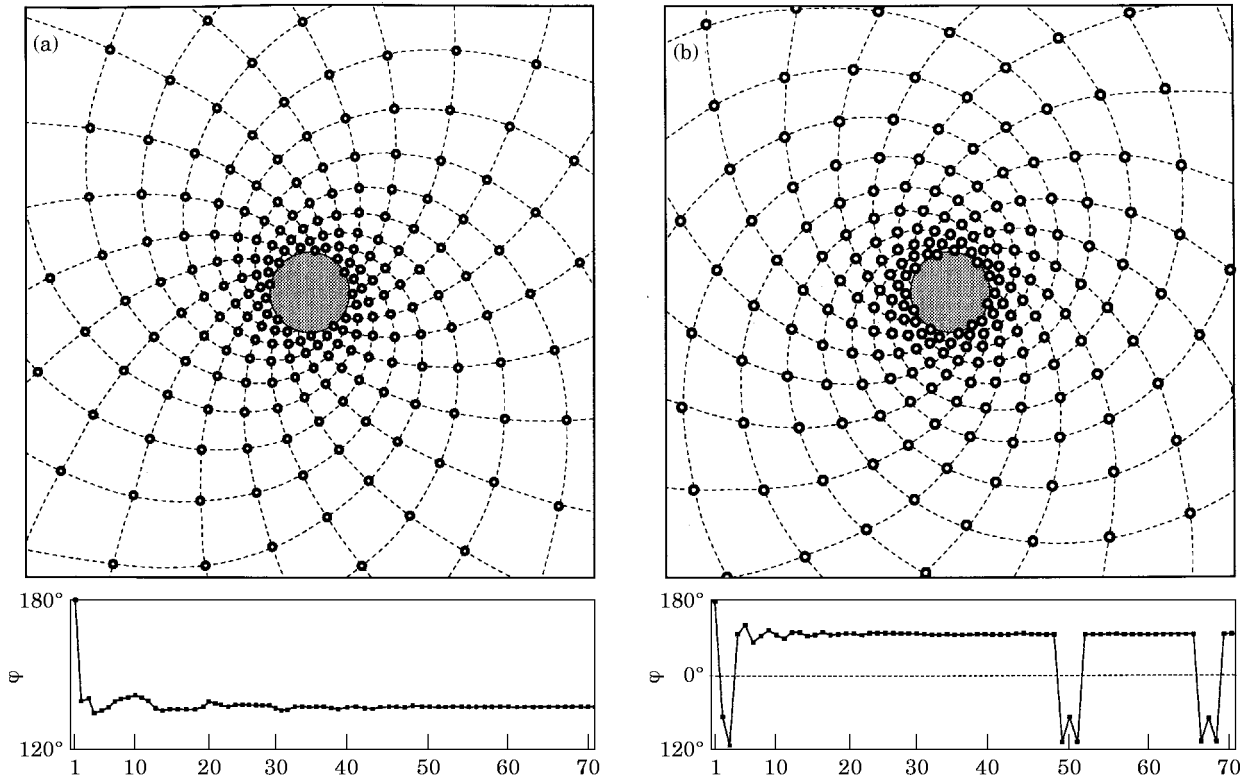


FIG. 5. Typical patterns obtained in the numerical simulation (with an exponential growth). The computed positions for the primordium centres are shown at a given instant with small circles (the parastichies and the apex radius were drawn for an easier visualization of the structure). At the bottom of each figure a plot gives the evolution of the divergence angle  $\varphi$  with the number of deposited particles. (a) Pattern obtained after a transient from  $G=1$  (distichous mode), to a constant value  $G=0.01$ , in a characteristic time of six plastochrones. The final divergence steady angle is  $\varphi_f=137.47^\circ$  and the parastichy numbers are (13, 21). The transient is clearly visible on the plot of the divergence: the first two particles are opposite each other, then the divergence converges quickly towards  $137.5^\circ$ . (b) Pattern with secondary organization (11, 18) of the Lucas series obtained after a transient in the value of  $G$  from an initial value  $G=0.3$  down to  $G=0.01$ . The steady divergence angle is  $\varphi_f=99.49^\circ$ . The plot of the divergence shows two anomalies where successive values  $\varphi \approx -162^\circ, -99^\circ$  and  $-162^\circ$  are observed. This corresponds to a permutation in the order of appearance of elements  $n$  and  $n+1$  (giving the sequence  $\dots n-1, n+1, n, n+2, \dots$ ). The successive measured divergences are thus  $\varphi_f, 2\varphi_f [2\pi], -\varphi_f, 2\varphi_f [2\pi]$ . The anomaly of the pattern resulting from these inversions is not visible.

For smaller values of  $G$ , the obtained regimes depend on the initial conditions used to run the simulations. Three types of conditions can be used:

- (1) An impulsive start, the simulation beginning directly at the studied value of  $G$ , with no initial elements.
- (2) An imposed transient condition using a continuous change of  $G$ . For botanical relevance, we start from a large value of  $G$  and then decrease it to a constant value.
- (3) A forced condition using a particular initial symmetry. We initially create an artificial pattern with a given number of particles, and observe whether it can keep growing. This allows the study of the limits of existence of all the possible steady solutions.

Figure 4 shows  $\varphi(G)$  for all the steady regimes that we could obtain in our simulations. The main feature of this diagram is that the number of different possible solutions increases with decreasing  $G$ . These solutions form disconnected curves in the diagram. Only one of these curves is continuous for all values of  $G$ ; all the others exist only below a limit value of  $G$ . For this reason, when initial conditions resulting from a continuous decrease of  $G$  are used, the resulting divergence is always on this main curve. Along this curve, when  $G$  tends to zero,  $\varphi$  converges oscillatingly towards  $\Phi$ . At a given value of  $G$ , the observed pattern has two parastichy numbers  $i$  and  $j$  (with  $j > i$ ) which are consecutive numbers of the Fibonacci series. Figure 5(a) shows a disposition obtained at  $G = 0.01$  where  $i = 13$  and  $j = 21$ . Inspection of the patterns obtained for decreasing values of  $G$  shows that near each extreme of the oscillation of the curve, the pattern becomes locally hexagonal so that three sets of parastichies can be observed:  $(i, j, i+j)$ . This corresponds to the value  $G_{ij}$  for which there is transition from the parastichy pair  $(i, j)$  observed at  $G \geq G_{ij}$  to the next  $(j, i+j)$  which exists at  $G \leq G_{ij}$ . The convergence of  $\varphi$  towards  $\Phi = 137.508^\circ$  results from these successive transitions.

The other solutions on the secondary curves of Fig. 4 can be reached when a small value of  $G$  is imposed directly at the initial time. These secondary curves have a structure similar to the main one: along each of them a succession of bifurcations is observed, having the same rules of transition from  $(i, j)$  to  $(j, i+j)$ . They also correspond to Fibonacci types of series, the difference being that they are built with different initial terms. For instance, the second possible branch corresponds to the Lucas series, which starts with 1 and 3:  $\{1, 3, 4, 7, 11, 18, \dots\}$  Fig. 5(b) shows a pattern obtained on this branch at  $G = 0.01$  with parastichy

order  $(i = 11, j = 18)$  and  $\varphi = 99.49^\circ$ . Each of the branches of the diagram shown on Fig. 4 converges towards one of the irrational angles ( $99.502^\circ, 77.955^\circ, 151.135^\circ$ , etc.) related to the golden mean, listed by Bravais & Bravais (1837). In order to investigate the limits of existence of each solution, we forced initial artificial patterns and observed whether they could keep growing. Using this technique we found that, except for the main one, all the curves shown on Fig. 4 are interrupted above a limiting value of  $G$ . At this limiting point, a particular parastichy can be observed, say  $(i, i+j)$ . It can then be noted that the point for which this secondary curve ceases to exist is always in the  $\varphi(G)$  diagram close to the point  $\varphi(G_{ij})$  of another curve, where there is a transition from  $(i, j)$  to  $(j, i+j)$ .

For very small  $G$  and an impulsive start, the system undergoes long transients. It can converge on a steady regime with a constant divergence angle corresponding to one of the solutions described above. But in most cases it generates a periodic repetition of a sequence of different divergence angles (the smaller  $G$ , the longer the periodicity). In most cases however, the resulting pattern is similar to a regular pattern with only permutations of the appearance order of some primordia. An example of such permutations is seen on the bottom of Fig. 5(b). We will return to this problem in Section 5.4.

More complex patterns can also be observed. Their parastichy orders can be for instance of the type  $2(i, j)$  so that the spatial pattern looks like a bijugate mode (Douady & Couder, 1993). These cases are imperfect because, unlike in the botanical situation, the primordia cannot appear exactly at the same time (by construction of the model). They do, however, mark the proximity of other possible types of organization that will be reached when the rules proposed by Snow & Snow are used (Douady & Couder, 1996a, b).

Finally, we can note that sets of simulations were performed with different interaction laws  $E(d) = 1/d, 1/d^3$  or  $\exp(-d/l)$  and with different  $V(r)$  dependence. Other simulations were also performed in conical and cylindrical geometries (for details on these geometries, see Part II). In all cases a  $\varphi(G)$  diagram having the structure shown on Fig. 4 was obtained. Changing any of these factors only affects the quantitative values of the thresholds  $G_{ij}$  and the shape of the curves near these transition points [Fig. 4(b)].

#### 4.3. DISCUSSION

The structure of Fig. 4 can be compared with diagrams based on geometric arguments which were

first derived by van Iterson (1907) when he produced phyllotactic patterns by paving a cylinder, a cone or a plane with hard disks. Most of van Iterson's diagrams are rather similar to those, examined in part II, which give the divergence as a function of the size of the primordia. Here, however, a diagram between  $\varphi$  and  $G$  and based on geometry can be obtained by stating that the new particle  $n$  is equidistant from the two previous particles of appearance order  $n-i$  and  $n-j$ . This is a good approximation in the case of a stiff interaction (i.e. with a potential energy decreasing rapidly with  $d$ ). The potential then only depends on the closest particles, and it is smallest along the mediatrix of the segment joining them. This approximation reduces our dynamical energetic problem to a geometrical one and gives a relation between  $\varphi$  and  $G$  for each given pair  $(i, j)$  of parastichies. In order to achieve this calculation we assume that the regime is stable with a constant divergence  $\varphi$ . We take as an origin the formation of a primordium of appearance order  $n$  at the position  $r = R_0$ ,  $\theta = 0$  (in polar coordinates). The position of a previous primordium of order  $(n-q)$  is then given by  $r = R_0 \exp(qG)$ ,  $\theta = q\varphi$ . Writing that the primordium of order  $n$  is equidistant from primordia  $n-i$  and  $n-j$  provides a relation between  $\varphi$  and  $G$ :

$$\exp(2iG) - \exp(iG) \cos(i\varphi) = \exp(2jG) - \exp(jG) \cos(j\varphi).$$

For each given pair of parastichies  $(i, j)$  this relation gives a  $\varphi(G)$  dependence similar to that derived by van Iterson paving a plane with exponentially growing disks. These divergences are drawn in Fig. 4 (thin continuous lines). In this geometrical model, as in all related geometrical models, the curve corresponding to parastichies  $(i, j)$  (with  $j > i$ ) is connected at  $G_{ij}$  with the two curves  $(j, i+j)$  and  $(i, i+j)$ . The geometrical model gives an analytic prediction for the values  $G_{ij}$  of the successive thresholds (for instance the first threshold occurs at  $G_c = \text{Ln}[2] \approx 0.693$ ). Two remarks are essential.

- (1) If a very stiff type of interaction is used (e.g.  $E(d) = \exp[-r/l]$ ) the values of  $\varphi(G)$  obtained dynamically can be extremely close to those obtained in the geometrical model [see Fig. 4(b)].
- (2) Qualitatively, however, the dynamical diagrams always differ from the geometric ones by an essential feature: at the bifurcation near  $G_{ij}$  the segment of curve  $(i, j)$  is only linked with  $(j, i+j)$ , while the curve  $(i, i+j)$  appears as a new disconnected branch. Only one continuous transition, from  $(i, j)$  to  $(j, i+j)$ , is thus possible.

In two recent articles Levitov (1991a, b) investigated a minimum energy condition on helical lattices. His work can be seen as a continuation of van Iterson's but with an additional optimization condition. In a periodic cylindrical geometry he assumed a regular lattice with repelling elements, and looked at the lattice slope for which the interaction energy is minimum. He showed that the compression of the whole lattice produces a similar diagram also with imperfect bifurcations. This theoretical work is further from botanical reality, but the similarity of his  $\varphi(G)$  diagram with ours is striking. It shows that the dynamics of the appearance of the new primordium at the place of lowest repulsive energy, creates a final structure corresponding to a minimum of the global interaction energy. This coincidence is similar to the relation which exists in crystallography between the investigation of the energy of periodic structures and of their growth mechanism. The geometrical reason from which Levitov obtains disconnected branches is, however, different from our dynamical one (Douady, 1994).

## 5. The Relevance to Botany of the Experimental and Numerical Results

The results presented above give an understanding of several characteristics of plant growth if the temporal variation of  $G$  during ontogeny is taken into

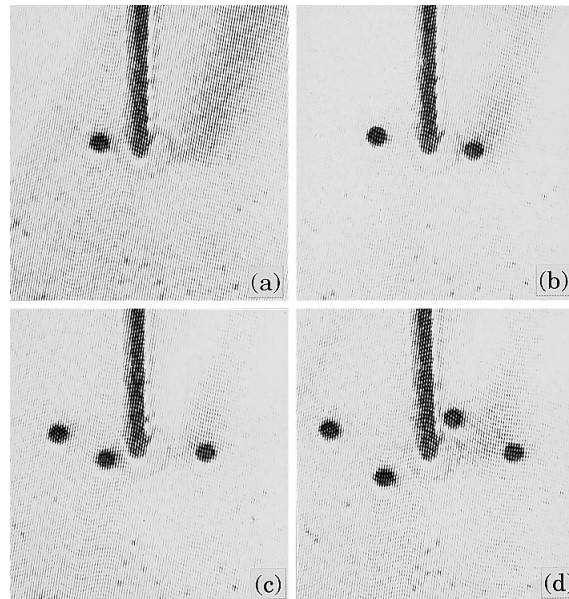


FIG. 6. Four successive photographs of the experiment showing the initial transient process with the formation of the first two elements in a distichous position, the symmetry breaking at the third, and the resulting formation of a spiral mode.

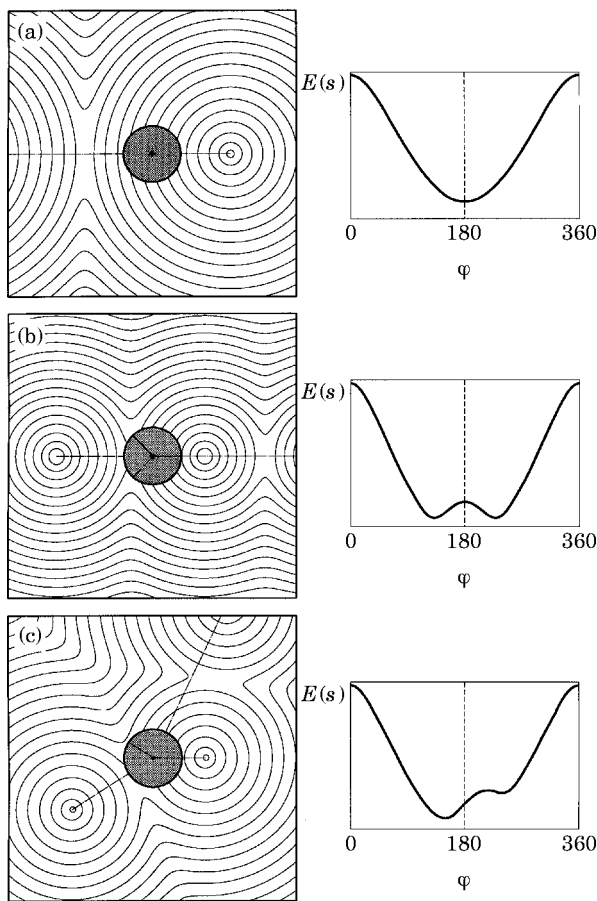


FIG. 7. The breaking of the alternate symmetry in the simulation. The figures to the left show the position of the particles and the resulting equipotential lines. To the right are drawn the resulting values of the potential on the central circle as a function of the angular position  $\varphi$ . (a) For  $G > G_c$ , there is only one minimum and the incipient particle will appear in a position opposite the previous one (distichous model). (b) Situation for  $G < G_c$  when the third particle is about to be formed. The first two particles create a potential with two equivalent minima on each side of the axis. The third particle will appear in either of these places. (c) Situation for  $G < G_c$  after the formation of the third particle. The potential has lost its symmetry so that the two potential wells are no longer equivalent; the position of formation of the fourth particle is entirely determined. This situation is identical for all the particles to be formed later. The third particle thus determines the direction of rotation of the generative spiral.

account. We will show this botanical relevance for four well-known characteristics of phyllotaxy:

- (1) The equal probability of the formation of generative spirals in both directions (Beal, 1873; Allard, 1946).
- (2) The predominance of the main Fibonacci series in the parastichy orders, and the transitions for which there exist quantitative data.
- (3) The possibility of exceptions with parastichy orders in secondary Fibonacci series.

- (4) The complex structure of the inflorescence of compositae.

We will also discuss four particular situations.

5.1. THE INITIAL BREAKING OF THE SYMMETRY

Let us consider here the simplest initial growth of a seedling and examine the position of the first few leaves. We will, for the time being, assume that there is no initial asymmetry in the system. The first leaf will thus form in a direction determined at random, this being the first breaking of symmetry of the system. If the growth occurs with a plastochrone ratio  $G > G_c$  then the leaves will successively grow in alternate positions. If  $G$  is smaller than  $G_c$ , the system will undergo a transition to a spiral mode. The experiment and the simulation permit the observation and the understanding of this transition. Figure 6(a-d) shows the position of the first drops in an experiment performed at  $G = 0.3$ . The second drop, being repelled only by the first one, will form in the opposite position, but the third drop breaks the symmetry and gives the system its chirality. All the following elements have no choice and position themselves along a spiral. The same phenomenon is observed in the simulation and can be described in more detail. In Fig. 7 we have drawn the isopotential due to the repulsion of the first two drops, respectively, in the cases  $G > G_c$  Fig. 7(a) and  $G < G_c$  Fig. 7(b). The potential  $E(s)$  along the central circle's perimeter [Fig. 7(a)] has a single minimum at  $\varphi = 180^\circ$ , showing that for large values of  $G$  only the alternate mode is possible. In contrast, for  $G < G_c$  [Fig. 7(b)] the repulsion caused by the first particle is no longer negligible and  $E(s)$  presents a symmetrical double well. Random influences will decide in which of the two possible positions the third particle will be placed. This breaking of the symmetry is irreversible; the potential well that the fourth particle (and all the later ones) will form has become asymmetrical [Fig. 7(c)] so that there is no longer a choice.

Returning to the plant, this means that the critical event is likely to be the growth of the third leaf following a decrease of  $G$  below  $G_c$ . The position of this primordium, which can appear at random in one of two equivalent positions, will irreversibly determine the direction of the winding of the generative spiral. This has already been suggested by Sachs (1991).

In most botanical cases, however, the production of the first elements does not occur in a perfectly axisymmetric environment because from the start a shoot has lateral appendages such as cotyledons. We will take these factors into account in Part III

(Douady & Couder, 1996b) and show that the random character of the choice persists. It explains that in the main stems of spirally growing plants there is an equal probability of finding left and right hand generative spirals (Beal, 1873; Allard, 1946).

## 5.2. THE PREDOMINANCE OF THE MAIN FIBONACCI SERIES

Ever since the early works of Schimper (1830), Braun (1831) and Bravais & Bravais, (1837a, b) the measurements performed on spirally organized botanical elements have shown that most of the parastichy orders are elements of the main Fibonacci series. After the introduction of the plastochrone ratio  $a$  by Richards (1951), several quantitative measurements investigated experimentally the relation between the value of  $a$  and the observed phyllotaxy in the apical region. In all these works a relation between the evolution of the phyllotactic order and the time evolution of  $a(t)$  was demonstrated. This evolution occurs spontaneously during the growth of the plant. The works of Schwabe (1971), Williams (1975), Erickson & Meicenheimer (1977) and Meicenheimer (1987) clearly defined the decrease of  $a(t)$  [or  $G(t)$ ] during the ontogeny from a seedling to the vegetative regime, and from vegetative to flowering, and demonstrated the corresponding increase of the parastichy order. In contrast, in other types of experiments, changes of the plant's phyllotactic organization were artificially induced by a chemical treatment of the vegetative shoots (Maksymowych & Erickson, 1977; Meicenheimer, 1979) or by photoperiodic floral induction (Erickson & Meicenheimer, 1977). These changes could also be directly ascribed to a simple change of the plastochrone ratio. In some of these measurements (Maksymowych & Erickson, 1977; Erickson & Meicenheimer, 1977; Lyndon, 1978) the evolution of the parastichy order and of  $\varphi$  were compared with corresponding values expected from van Iterson's diagrams. The agreement of the former was more convincing than that of the latter, possibly because the measurements were done during transient regimes. These botanical experiments demonstrated that, from the phyllotactic point of view, the main dynamical characteristic is the continuous evolution of the plastochrone ratio with time. As the older parts create the conditions for the later growth through the iterative appearance of the primordia, the phyllotactic pattern depends on the whole history of its growth. We can note that the evolution of a given apical meristem in real time can now be watched using the technique introduced by Green *et al.* (1991), which should be a useful tool as it permits direct observation of the iteration.

The best defined patterns are those produced by the plant during periods where the plastochrone ratio remains constant. For instance, during the growth of a stem the plant can produce a large number of leaves in identical conditions. Similarly the inflorescences with the best defined spiral structures are those with a large number of identical elements. It must be kept in mind, however, that these steady regimes are always reached after a transient. In the experiment as well as in the simulation the best way to reach botanically relevant patterns at a fixed value of  $G$  is to start at a large value of  $G$  and then decrease it progressively to a constant value. With such transients, even if they are short, we always obtain patterns with parastichy order  $i$  and  $j$  consecutive terms of the main Fibonacci series. For instance, the

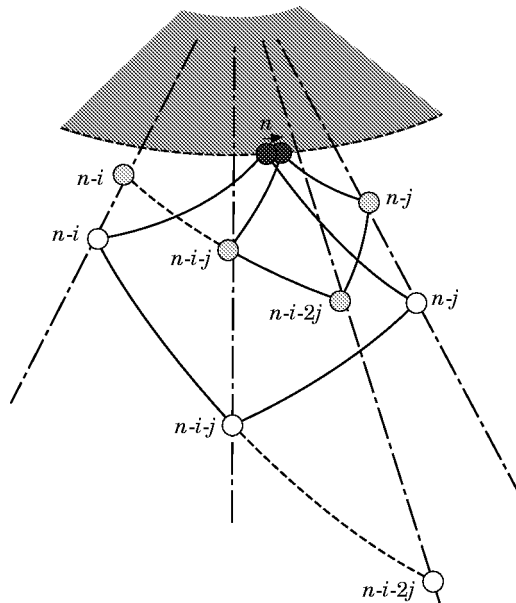


FIG. 8. Sketch of the positions of the neighbours of an incipient particle. The new particle has an appearance order  $n$  and is shown in black. The first configuration shown here (with particles drawn as open circles) corresponds to a value of  $G$  where the parastichy order is  $(i, j)$ . It is known from the periodicity rules that in this case the neighbours of primordium  $n$  have appearance number  $n-i$  and  $n-j$ . It is the repulsion of these two particles which determines the exact position of  $n$ . We can note that the primordia  $[n, n-i, n-i-j, n-j]$  form approximately a rhomb. As  $n-j$  is older than  $n-i$  ( $i < j$ ), this rhomb is inclined relative to the radial line passing by  $n$ . If the factor  $G$  is reduced (say by decreasing the advection velocity  $V$ ) the particles move a smaller distance away from the apex so that their relative positions are changed. The important feature is that the distance between element  $n$  and element  $n-i-j$  decreases. At a value  $G_0$  (not shown here) the element  $n$  will become equidistant from  $n-i$ ,  $n-j$  and  $n-i-j$ , and the pattern will be locally hexagonal. At this point the repulsion caused by particle  $n-i-j$  is no longer negligible. Because of the asymmetrical position of the rhomb, it will tend to push  $n$  in the direction given by the arrow. When  $G$  is further reduced the pattern shown in grey dots will be reached. The two neighbours of the new primordium  $n$  have become spontaneously  $n-j$  and  $n-i-j$ ; it is their repulsions which now determine its position.

steady regime displayed on Fig. 5(a) was obtained from initial distichous elements by an exponential decrease of  $G(t)$  having a characteristic time of six iterations. This result is a generalization of a similar convergence that had been obtained respectively by Mitchison (1977) in a simulation of inhibitor diffusion in a cylindrical geometry and by Williams & Brittain (1984) in purely geometrical simulations.

To understand this result, the key point is that the whole diagram  $\varphi(G)$  (Fig. 4) is formed of non-branching continuous curves. The predominance in botany of the Fibonacci series can be derived from this particularity, and from the usual growth conditions in plants. As  $G$  decreases during the shoot's growth, there is only one continuous way through all the successive bifurcations; along this way the divergence converges towards  $\Phi$  and the parastichy numbers follow the Fibonacci series.

It is, therefore, an essential feature that at each threshold  $G_{ij}$ , there is continuity between the mode  $(i, j)$  and the mode  $(j, i+j)$  while the mode  $(i, i+j)$  appears disconnected. There is an intuitive way of understanding what occurs at such a threshold. Above  $G_{ij}$ , the new particle  $n$  appears roughly equidistant from  $n-i$  and  $n-j$  (Fig. 8). Its exact position results mainly from the repulsion of  $i$  and  $j$ , and the role of the other  $j$  latest particles is only to prevent the possibility of appearance at other sites around the apex. If no particles other than the  $j$  latest were ever taken into account, for  $G$  tending to zero the divergence would tend monotonically towards a rational value  $[2\pi/(i+j)]$  and  $n$  would appear at the same angular position as  $n-(i+j)$ . In fact, long before reaching  $G=0$ , near  $G_{ij}$ , the repulsion caused by this element of order  $n-(i+j)$  is no longer negligible and  $n$  slides to avoid it. The situation at this point is not symmetrical: above  $G_{ij}$  the element  $n$  is always angularly situated between  $n-(i+j)$  and  $n-j$  (Fig. 8). Below  $G_{ij}$ ,  $n$  thus slides between  $n-j$  and  $n-(i+j)$  and this corresponds to the selection of the transition. In the geometrical models, the situation is the same, but  $n$  is allowed to slide on both sides of  $n-(i+j)$ , because a geometrical approach only assumes the positioning of the new element between two older ones, so that it corresponds to a minimum of the potential. In our model, the condition that this position should be the best, i.e. the absolute minimum, is added. As  $n-j$  is older than  $n-i$ , it is clear that below  $G_{ij}$ , the possible position between  $n-j$  and  $n-(i+j)$  has a lower potential than between  $n-i$  and  $n-(i+j)$  (Fig. 8). The same fundamental selection would be obtained in a geometrical model if a dynamical criterion of choice for the position of the new particle was added (Douady, 1996).

It is possible to reach an intuitive understanding of this self organization by a simple argument. Let us consider the system at a value of  $G$  corresponding to the branch  $(i, j)$ . At this value the position of a new particle is determined by the repulsion of the  $j$  most recent elements. Let us suppose for a moment that all the older elements have had their repulsive potential artificially switched off. Then, as  $G$  is reduced, there will be no bifurcation and the  $(i, j)$  branch will be followed all the way down to  $G=0$ . The angle that will be reached at  $G=0$  will be rational. For instance an organization  $(1, 1)$  will lead to  $\varphi = 180^\circ = (1/2)2\pi$ ;  $(1, 2)$  to  $\varphi = 120^\circ = (1/3)2\pi$ ;  $(2, 3)$  to  $\varphi = 144^\circ = (2/5)2\pi$ ;  $(3, 5)$  to  $\varphi = 135^\circ = (3/8)2\pi \dots$ , more generally a branch  $(i, j)$  will tend towards  $(p/i+j)2\pi$  where  $p$  is an integer called the encyclic number associated to  $i+j$  (Bravais, 1837). The specificity of these organizations is that when  $G$  tends to zero all the elements tend to be aligned on  $i+j$  radial lines (ortostichies). The new element (of order  $n$ ) thus tends to be radially aligned with the older element of order  $(n-i-j)$  and extremely close to it. In reality this is not possible because the repulsive potentials are not switched off and they forbid this proximity. The bifurcation  $(i, j)$  to  $(i, i+j)$  is the reaction of the system that prevents this proximity. The successive bifurcations can thus be seen as a sequence of "repulsions" by rational organizations. The convergence towards an irrational angle naturally results from the avoidance of successive rationals.

The overwhelming predominance of the Fibonacci series in botany can be derived from this result, and from the fact that usually the evolution  $G(t)$  of the plastochrone ratio with time is continuous and starts from large initial values where only the main solution exists.

### 5.3. THE EXCEPTIONS TO FIBONACCI

Rare exceptions to this rule were first listed by Bravais & Bravais (1837a, b). Of most common occurrence are the bijugate phyllotactic modes where  $i$  and  $j$  are twice numbers of the main Fibonacci series. They are associated with the decussate modes of growth and they will be interpreted in Parts II and III (Douady & Couder, 1996a, b). The existence of members of secondary series was also noticed by the Bravais brothers. Data about their relative frequencies can be found in Jean (1994) and references therein. The most frequent amongst these exceptions are parastichy orders  $(i=4, j=7)$  or  $(i=7, j=11)$  which are related to the Lucas series built as the Fibonacci series, but with initial terms one and three (the divergence angle then tending towards  $99.502^\circ$ ). Less frequently they also found parastichy orders

( $i=5, j=9$ ) related to the series with initial terms one and four (the limit divergence angle being  $77.955^\circ$ ) or parastichy orders ( $i=5, j=7$ ) corresponding to the series with initial terms two and five (the divergence being close to  $151.135^\circ$ ).

As noted earlier, we find the possible spontaneous formation of these modes when the transient leading to small  $G$  is very short or when the simulation is started directly at a low value of  $G$ . We observed that the best way to obtain a pattern on a secondary branch ( $i, i+j$ ) is to start directly at value of  $G$  in the vicinity of  $G_{ij}$  but below it, a region where this new branch starts to be possible. For instance, the mode ( $i=11, j=18$ ) shown on Fig. 5(b) was obtained after a transient starting from  $G=0.3$ , a value for which, without any previous particles, the system stabilizes directly in the ( $i=1, j=3$ ) solution. The system thus started on this branch and remained on it when  $G$  was decreased. This corresponds to the common observation that when a sunflower inflorescence follows the Lucas series its leaves already grow on this secondary branch with a divergence angle close to  $99^\circ$ . We will return to this point in Part III.

The other possibility for a plant to reach an anomalous mode is that an external perturbation generates a local necrosis of the apical meristem disturbing the iteration. We observed such a transition on a branch of a pine tree. It was bent locally, showing that it had undergone a perturbation during the growth. At this level the phyllotaxy underwent a transition from (3, 5, 8) to the multijugate spiral (4, 8). Such transients were obtained artificially by Snow & Snow (1962) by microsurgery of the apical meristem.

#### 5.4. THE COMPLEX STRUCTURE OF THE INFLORESCENCES OF COMPOSITAE

We can finally consider the spectacular ordering of sunflower heads (Weisse, 1897; Richards, 1948; Ryan *et al.*, 1991). Inspection of the whole plant shows the continuity of the generative spiral along which, successively, leaves, bracts, ligulae, and then florets have formed. As for the parastichy orders they first increase following the rule ( $i, j$ ) to ( $j, i+j$ ) to reach a maximum at the periphery of the inflorescence. Remarkably high Fibonacci numbers can be reached in this region (e.g.  $i=144, j=233$ ). The reverse evolution is observed in the inflorescence itself. Following a parastichy of the highest order  $j$  from the periphery inward, it appears to be interrupted by a change of order before the centre is reached. All the parallel parastichies of order  $j$  undergo the same transition at approximately the same distance from the centre (Richards, 1948). In contrast the paras-

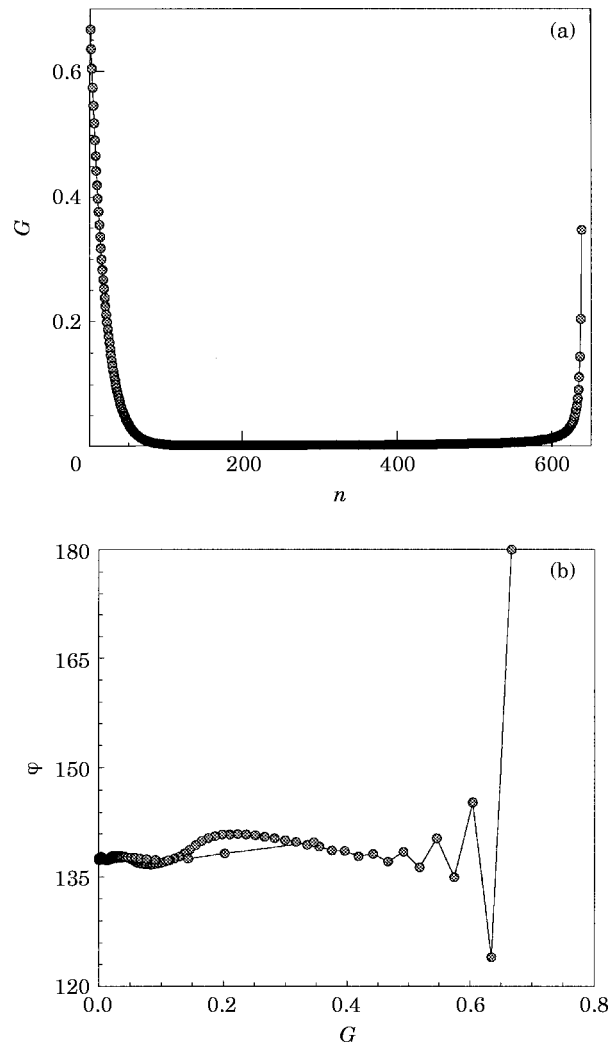


FIG. 9. Simulation of a sunflower head with 500 florets. (a) The imposed time evolution  $G(n)$ ,  $n$  being the number of the deposited particle. It is first decreased from 0.7–0.005 and then increased back to 0.3. (b) The resulting evolution  $\phi(G)$  showing the oscillating convergence of  $\phi$  towards  $\Phi$  as  $G$  is decreased. During the final increase of  $G$  the values of  $\phi$  follow a slightly different path because of the inertia of the system.

tichies of order  $i$  remain continuous in this region. This corresponds to the annular region where the patterns undergo transitions of the type ( $i, j$ ) to ( $j-i, i$ ) (the normal transitions taken in reverse). A geometrical analysis of these transitions in terms of crystallographic defects can be found in Rivier (1988) and Rothen & Koch (1989). This evolution can be reproduced dynamically in the numerical simulation if a time evolution of  $G(t)$  is introduced, corresponding to the evolution of the plastochrone ratio during the whole of the plant's growth. The transition from a vegetative to a flowering apex corresponds to a decrease of  $G(t)$  because of the simultaneous slowing down of the growth, the decrease of the plastochrone and the increase of the apex size (Lyndon, 1990). With

the completion of the flower head the growth stops; in this process, as the apex shrinks  $G(t)$  increases. We did a simulation of this type of growth using the  $G(t)$  dependence, shown in Fig. 9(a).  $G$  first decreases from one down to a very small value ( $G=0.001$ ), corresponding to a transition from the first leaves to the first florets. At the end of the growth  $G$  increases back satisfying:

$$G(n) = 1/2 \text{Ln}[(N-n+1)/(N-n)],$$

where  $N$  is the total number of florets in the inflorescence, and  $n$  the incipient floret number. This particular law was chosen so that, even with exponential growth, the final aspect of the simulation would correspond to a constant surface density of florets. The time evolution of the resulting divergence angle is shown in Fig. 9(b). Three successive states of the spatial patterns are shown in Fig. 10: the first particles [Fig. 10(a)] have angular positions of the leaves and bracts. With the decrease of  $G$  the highest phyllotactic orders are then reached corresponding to the formation of the periphery of the inflorescence [Fig. 10(b)]. As  $G$  increases back the reverse transitions between parastichy orders  $(i, j)$  to  $(j-i, i)$  are observed [Fig. 10(c)], corresponding to the well known inner structure of the inflorescence (Bravais, 1837; Weisse, 1897; Richards, 1948; Rivier, 1988).

This simulation, as it leads to the formation of very high Fibonacci orders, can become unstable. The first type of destabilization is observed if we record the divergence angle as a function of time. While the iteration was perfect in the case shown on Fig. 9(b), in other cases successive values of  $\varphi$  can be very different from each other [Fig. 11(a)]. It is to be noted that such perturbations remain practically invisible on the resulting pattern [Fig. 11(b)]. This can be understood by close inspection of the  $\varphi(n)$  recordings [Fig. 11(a)]. All the successive values of divergence angles are of the type  $p\varphi$  or  $p\varphi \pm 2\pi$  where  $p$  is a non-zero positive or negative integer. This shows that, as in the case of Fig. 5(b), the anomalies correspond to complex permutations in the appearance order of successive elements. These permutations destroy the generative spiral: the line linking the elements in their order of appearance now runs back and forth around the stem. The parastichies are, however, only weakly affected, because these anomalies do not disturb the angular order and only induce small disturbances in the radial position of the elements. This result is interesting as it shows the stability of the pattern formation: for small  $G$ , the regularity of the order of appearance is not very important. It is the local

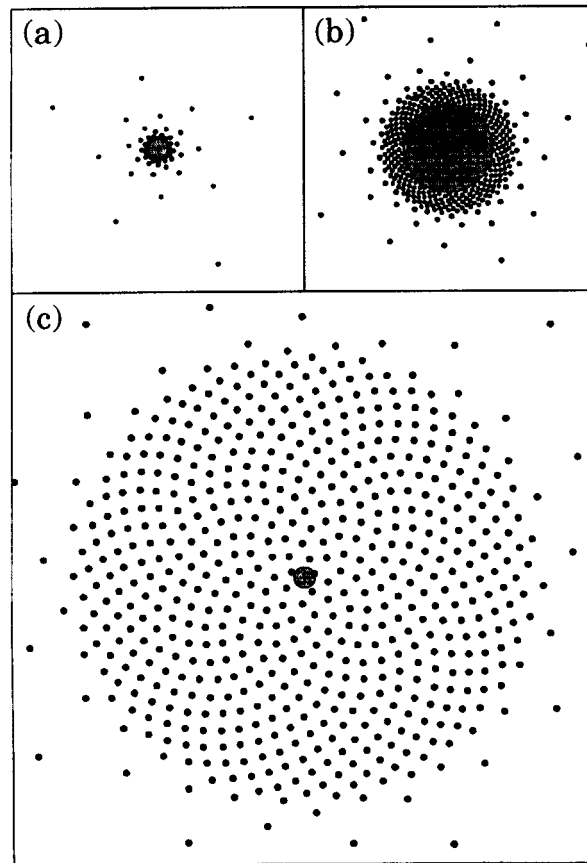


Fig. 10. Patterns obtained successively at three stages of the simulation of Fig. 9: (a) An early stage where  $G$  has already 39,6 decreased to its minimum value corresponding to the end of the vegetative growth, and the formation of the first florets. The divergence is already close to  $\Phi$ . (b) An enlarged view of the inflorescence bud. Half of the florets have been formed on the border, which present the higher parastichy numbers, here (34, 55). The equivalent of the transition from the bractae to the florets is clearly visible. (c) The final increase of  $G$  generates the decrease of the parastichy numbers from the border to the centre of the flower, thus reproducing the observed patterns.

order around each primordium that is important, and it is preserved even if the formation order becomes irregular.

If the first decrease of  $G$  is too brutal, however, or if too large a noise is introduced,  $\varphi(n)$  becomes completely chaotic and destabilization of the pattern is observed [Fig. 12(a)]. Such disorder was observed by Hernandez & Palmer (1988) in an experiment where they operated the receptacle surface so as to isolate the central region. In this region, where the formation of primordia started at very low  $G$  without the influence of previous elements, disordered patterns were obtained. Such disorder is sometimes seen in the central region of sunflowers, and very often in *Chrysanthemum* flowers sold commercially, possibly because of the various artificial treatments to

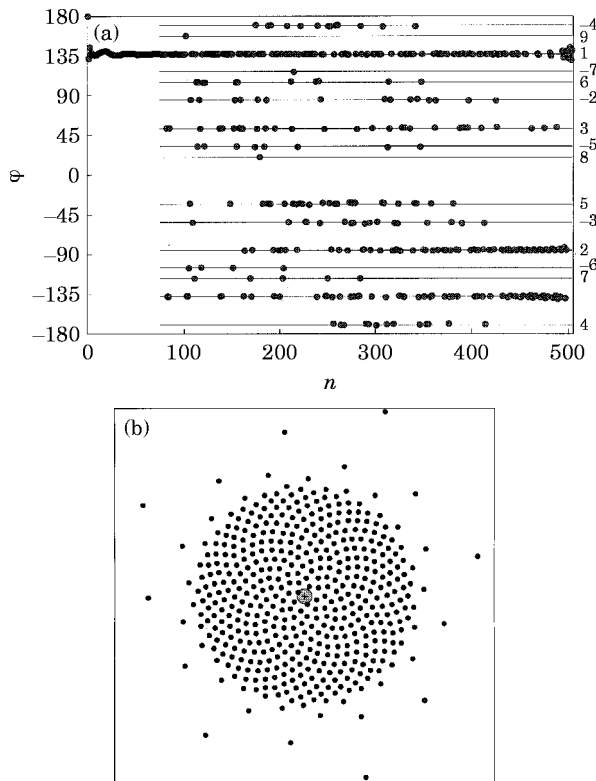


FIG. 11. Simulation similar to that of Figs 9 and 10 showing a weakly disordered situation obtained during a faster decrease of  $G$ . (a) Plot of the angle  $\varphi$  between two successive elements as a function of the element's order. This angle is no longer constant but all the observed values are of the type  $\varphi' = p\Phi$  (modulo  $2\pi$ ), where  $p$  is an integer (the values of  $p$  are given on the right of the plot). This apparent disorder only corresponds to permutations in the order of formation of the elements, similar to those shown in Fig. 5(b) [the maximum number  $p$  possible without disrupting the structure is simply related to the parastichy numbers, it is roughly  $(j-i)$ ]. (b) The corresponding spatial pattern. The disturbances due to permutations of the order of formation are not visible.

which they were submitted [Fig. 12(b)]. It is to be noted that if the system, while  $G$  is small, jumps to a secondary series, when  $G$  increases back it has no way of evolving continuously because the branch is interrupted. Once again, the normal Fibonacci structure is the only one where all the transitions, for both decreasing and increasing  $G$ , are always regular and occur without disruption of the structure.

#### 5.5. DISCUSSION OF FOUR SPECIFIC BOTANICAL OBSERVATIONS

Finally, before concluding, four specific observations need to be clarified in the framework of this article.

(1) On many branches of trees there is continuity of the phyllotaxic pattern over several years. How can this continuity exist in spite of the dormant winter periods? We can note that our parameter is determined by the product of  $T$  with  $V$  so that it

can remain constant even when  $V$  tends to zero, provided  $T$  grows as  $1/V$ . This will have obvious causes in the simulations with the principles of Snow & Snow.

(2) In their precise measurements of the leaf positions on mature stems, Bravais & Bravais (1837) found values of  $\varphi$  very close to the ideal angle  $\Phi$ , even in the case where the parastichy numbers were very small (e.g.  $i=2$ ,  $j=3$ ). This observation later generated a long lasting hypothesis that the plants form their elements at the perfect divergence angle  $\Phi$ . In this hypothesis the parastichy organization only reveals successive rational approximations of an underlying ideal irrational organization.

In fact, to each observed parastichy order  $(i, j)$  corresponds a range of possible values of  $\varphi$ . Because of the oscillation of the main curve of Fig. 4 the particular value  $\varphi = \Phi$  always lies within the ranges of each of the orders  $(i, j)$  of the main Fibonacci

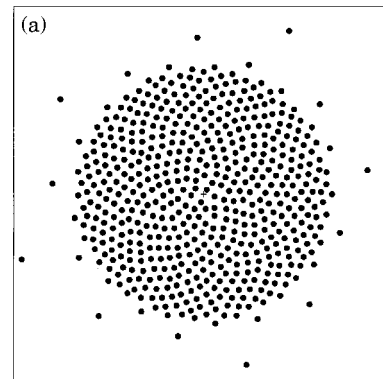


FIG. 12. (a) Simulation similar to Fig. 11 with a faster decrease of  $G$  leading to a strongly disordered situation. The smaller number of bracts around the inflorescence is due to this rapid decrease. (b) Photograph of a disordered commercial *Chrysanthemum*.

series. If for high parastichy order the range of values is narrow, it can be very wide for low orders: for instance, an organization ( $i = 1, j = 2$ ) can be found for any value  $180^\circ > \varphi > 128^\circ 10'$  (van Iterson, 1907; Adler, 1974). For this reason it might appear surprising that the measurements performed on mature stems (as done by Bravais & Bravais, 1837a) show values of  $\varphi$  close to  $\Phi$  even in the case of low parastichy order. These observations can be understood as resulting from the difference of organization near the apical meristem and along the stem. This difference is because of the extension of the internode in a long shoot type of growth. In this process the angular positions of the primordia remain unchanged but the pattern is stretched longitudinally. This is clearly seen on Fig. 13 showing an *Asparagus* shoot: the primordia are more tightly packed in the region of the tip than further along the stem. The parastichy order ( $i = 5, j = 8$ ) observed at a macroscopic scale on this photograph in the tip region is identical to the order of the primordia at the

periphery of the apex as revealed by dissection. But further down the stem the pattern is stretched and the order of the conspicuous parastichies is decreased (to e.g.  $i = 2, j = 3$  on Fig. 13). The divergence  $\varphi$  determined in the apical region ( $138^\circ 8' > \varphi > 135^\circ 55'$  for a mode  $i = 5, j = 8$ ) retains along the stem a value much closer to  $\Phi$  than apparently needed by the low order of the parastichies ( $142^\circ 6' > \varphi > 128^\circ 10'$  for a mode  $i = 2, j = 3$ ). As shown by Plantefol (1948) the original parastichies can be found on a mature stem by the observation of the contact parastichies of the foliar scales when they are visible. These parastichies can also be obtained by observation of the vascular traces in the stem.

The belief that the divergence angles are always close to an irrational angle can lead to errors. For instance, the secondary series starting with two and five has a limit angle  $151.135^\circ$ , but the measurement of an angle of divergence of the order of  $150^\circ$  should not be ascribed automatically to this type of solution. It is more likely to be a mode ( $i = 1, j = 2$ ) obtained at large values of  $G$  [as the pattern obtained in the experiment, shown in Fig. 3(b)]. In all cases a complete definition of the phyllotactic mode requires the measurement of  $a$ ,  $\varphi$  and of  $(i, j)$ , the order of the contact parastichies in the apical region.

(3) In some plants (in particular cacti), Fibonacci spirals are observed, but with a periodic arrangement and thus a rational divergence (in these plants there are both parastichies and well-defined orthostichies). In all the cases we know of, the stems have polygonal sections, suggesting that the axisymmetry of the shoot is broken. The rational arrangements of the primordia then result from the locking of their position by their interaction with this structure of the shoot. This is clearly visible in many cacti [e.g. *Echinocereus reichenbachii*, according to Boke (1950)] where the spines are located on the top of radial ribs.

(4) There are plants (e.g. *Costus*) in which the leaves form one single spiral with a divergence angle which can be small (spiromonostichous phyllotaxy). The structure of *Costus* was used by Plantefol (1948) as an argument to put forward his "foliar helices" hypothesis. This is an opportunity to discuss this theory. Plantefol suggested that the dynamically important structures for spiral phyllotaxy were what he called the foliar helices (which are simply the parastichies of one direction). His starting point was that the incipient primordium forms in the continuity of the existing parastichies. This is a valid description of what is visually observed and we can remark that the results of our experiments are compatible with Plantefol's description: even though the interaction is repulsive, we also see [Fig. 3(c)] each new element



FIG. 13. The tip of an asparagus stem showing that the internode's secondary growth induces by elongation a change of the parastichy order from (5, 8) in the tip region to a (2, 3) order further along the stem.

placing itself in the continuity of the existing parastichies. Using this observation Plantefol then proposed that there existed at the tip of these helices “generative centres” which repeatedly created the new primordia. In this model, however, there is nothing to determine the number of foliar helices, so the predominance of Fibonacci numbers in botany is not taken into account. Our results show that all the dynamical models where the new primordium forms in a position determined by either a repulsion or an inhibition from the previous elements will give rise to the organization of Fibonacci order. As discussed above, this effect is fundamentally linked with the system’s trend to avoid rational organization because of the repulsion or the inhibition between elements. This type of interaction, absent from Plantefol’s theory of generative centres, appears to be a necessary ingredient of any complete theory of phyllotaxis.

Returning to *Costus*, how can it have a single helix? The organization of a single spiral is impossible in our model. With the help of Professor R. Hebant, we performed dissections of apices of *Costus afer* and found that each primordium forms a sheath around the apex (as is common for monocotyledons) and has a very asymmetrical shape. This can be seen in several of the photographs of apices in Kirchoff & Rutishauser (1990). In *Costus*, therefore, the position of the available space appears to be defined directly by the specific shape of the previous primordium.

## 6. Partial Conclusions

The golden mean and the Fibonacci series both have very specific mathematical properties. These are translated into remarkable geometrical properties in the Fibonacci spiral lattices. For this reason, many researchers of the field have sought to explain the appearance of these lattices by their functional properties. In particular the fact that the divergence angle tends towards an irrational value is often thought of as being useful for the plant: the leaves along the stem are never exactly superposed so that their exposure to the sun is optimal. This appears to be oversimplified: it assumes that all stems are vertical and that the sun is always at the zenith. It also neglects the fact that the leaves can modify their orientation. For instance, in our latitudes, even a normal vertical pine tree branch, with a Fibonacci structure, exhibits anisophylly along the north–south direction. Furthermore, in this regard the very common decussate phyllotaxy should not exist as leaves in this mode of organization are superimposed.

The main drawback of this type of interpretation is, however, that it is finalistic. We do not deny that selective pressure can favour some organizations, however a mechanism for the formation of these various structures has to exist before the selective pressure chooses amongst them.

In the present article our aim was to demonstrate that the dynamical hypothesis put forward by Hofmeister (1868) formed the rule of an iterative system which produces the observed spiral structures. We showed that it was possible to obtain them in an analogous physical experiment and in a numerical simulation. The latter provided information about the steady regimes, the transients and the evolution of the pattern with the external control parameter. The process proved very robust, being independent of the chosen repulsive energy as well as of the velocity law.

The main result of this work is given by Fig. 4, which shows that for decreasing values of  $G$  the system undergoes a sequence of imperfect bifurcations through which, along the main branch,  $\varphi$  tends towards  $\Phi$ . Botanically, the predominance of the main Fibonacci series is linked with the fact that a new stem always starts to grow with a large plastochrone ratio in a range of values where only the main series exists. During the later growth, with the decrease of  $G$ , this branch will be followed steadily. The abnormal cases can be related either to a growth starting at a smaller value of  $G$  where the few observed, abnormal branches are possible, or to a local disturbance of the apex.

We have presented these partial results separately because their discussion is simpler in the framework of Hofmeister’s hypotheses. As noted above, however, this system does not lend itself to relating the spiral organizations and the whorled ones. For this reason the results of this first part, although they already lead to an understanding of many features, are based on too strong a hypothesis (an externally fixed plastochrone). The work of Snow & Snow (1952) provides another set of hypotheses. In the second part of this article (Douady & Couder, 1996a) we will see that they form the rules of a more general iterative system. In this new framework, all the results obtained here will be recovered, but a larger range of self organized patterns, including the whorled and multijugate modes, will become possible (preliminary results were given in Couder & Douady, 1993). In the third part of this article (Douady & Couder 1996b) we will study in which conditions the ontogeny leads either to a spiral or to a whorled phyllotaxis. Direct comparison of our results with botanical data will then become more precise and will be presented.

## REFERENCES

- ADLER, I. (1974). A model for contact pressure in phyllotaxis. *J. theor. Biol.* **45**, 1–79.
- AIRY, H. (1873). On leaf arrangements. (I) *Proc. R. Soc. Lon.* **21**, 176–179 and (II) (1874) *Proc. Roy. Soc. Lon.* **22**, 299–307.
- ALLARD, H. A. (1946). Clockwise and counterclockwise spirality observed in the phyllotaxy of tobacco. *J. Agr. Res.* **73**, 237–242.
- BEAL, W. J. (1873). The phyllotaxy of cones. *Amer. Nat.* **7**, 449–453.
- BOKE, N. H. (1950). Histogenesis of the vegetative shoot in *Echinocereus*. *Am. J. Bot.* **38**, 23–38.
- BRAUN, A. (1831). Vergleichende Untersuchung über die Ordnung der Schuppen an den Tannenzapfen. *Nova Acta Acad. Caesar Leop. Carol.* **15**, 195–402.
- BRAUN, A. (1835). Dr. Schimper's Vorträge über die Möglichkeit eines wissenschaftlichen Verständnisses der Blattstellung . . . *Flora. Iena*, **18**, 145–191.
- BRAVAIS, L. & BRAVAIS, A. (1837a). Essai sur la disposition des feuilles curvisériées. *Ann. Sci. Nat.* second series **7**, 42–110.
- BRAVAIS, L. & BRAVAIS, A. (1837b). Essai sur la disposition symétrique des inflorescences. 193–221, and 291–348; *Ann. Sci. Nat.* second series **8**, 11–42.
- BRAVAIS, L. & BRAVAIS, A. (1839). Essai sur la disposition des feuilles rectisériées. *Ann. Sci. Nat.* second series **12**, 5–14, and 65–77.
- CANNEL, M. G. R. (1978). Analysis of shoot apical growth of *Picea sitchensis* seedlings. *Ann. Bot.* **42**, 1291–1303.
- CHAPMAN, J. M. & PERRY R. (1987) Diffusion Model of Phyllotaxis. *Ann. Bot.* **60**, 377–389.
- CHURCH, A. H. (1904) *On the Relation of Phyllotaxis to Mechanical Laws*. London, Williams and Norgate.
- COUDER Y. & DOUADY, S. (1993). Phyllotaxis: genetic determination and self organization. In "Organisation et processus dans les systèmes biologiques". Friedel, J. & Gros, F. (eds). Paris: Technique et Documentation, Académie des Sciences.
- DOUADY, S. (1996). The packing efficiency of the phyllotactic patterns on a cylinder. Preprint.
- DOUADY, S. & COUDER, Y. (1992). Phyllotaxis as a physical self organised growth process. *Phys. Rev. Lett.* **68**, 2098–2101.
- DOUADY, S. & COUDER, Y. (1993). Phyllotaxis as a self organised growth process. In: *Growth Patterns in Physical Sciences and Biology* (Garcia Ruiz, J. M. et al. (eds). New York: Plenum Press.
- DOUADY, S. & COUDER, Y. (1996). Phyllotaxis as a self organizing process Part II: The whorled modes and their relation to the spiral ones. *J. theor. Biol.*, **178**, 275–294..
- DOUADY, S. & COUDER, Y. (1996). Phyllotaxis as a self organizing process Part III: The simulation of the transient regimes of ontogeny. *J. theor. Biol.*, **178**, 295–312..
- ERICKSON, R. O. (1973) Tubular packing of spheres in biological fine structure. *Science*, **181**, 705–716.
- ERICKSON, R. O. & MEICENHEIMER, R. D. (1977). Photoperiod induced change in phyllotaxis in *Xanthium*. *Am. J. Bot.* **64**, 981–988.
- GREEN, P. B. (1992). Pattern formation in shoots: a likely role for minimal energy configurations in the tunica. *Int. J. Plant. Sci.* **153** (3), S59–S75.
- GREEN, P. B., HAVELANGE, A. & BERNIER, G. (1991). Floral morphogenesis in *Anagallis*: scanning electron micrograph sequences from individual growing meristems before, during and after the transition to flowering. *Planta*, **185**, 502–512.
- HERNANDEZ, L. F. & PALMER, J. H. (1988). Regeneration of the sunflower capitulum after cylindrical wounding of the receptacle. *Am. J. Bot.* **75**, 1253–1261.
- HOFMEISTER, W. (1868). *Allgemeine Morphologie der Gewächse, Handbuch der Physiologischen Botanik*, 1 405–664. Leipzig, Engelmann.
- JEAN, R. V. (1984). *Mathematical Approach to Patterns and Form in Plant Growth*. New York: Wiley and Sons.
- JEAN, R. V. (1994). *Phyllotaxis, a Systemic Study in Plant Morphogenesis*. Cambridge: Cambridge University Press.
- KIRCHOFF, B. K. & RUTISHAUSER, R. (1990). The phyllotaxy of *Costus* (Costaceae). *Bot. Gaz.* **151**, 88–105.
- LEVITOV, L. S. (1991a). Energetic approach to phyllotaxis. *Europhys. Lett.* **14**, 533–539.
- LEVITOV, L. S. (1991b). Phyllotaxis of flux lattices in layered superconductors. *Phys. Rev. Lett.* **66**, 224–227.
- LYNDON, R. F. (1978). Flower development in *Silene*: Morphology and sequence of initiation of primordia. *Ann. Bot.* **42**, 1343–1348.
- LYNDON, R. F. (1990). *Plant Development, the Cellular Basis*. London: Unwin Hyman.
- MAKSYMOWYCH, R. & ERICKSON, R. O. (1977). Phyllotactic change induced by gibberellic acid in *Xanthium* shoot apices. *Am. J. Bot.* **64**, 33–44.
- MEDFORD, J. (1992). Vegetative apical meristems. *Plant Cell* **4**, 1029–1050.
- MEICENHEIMER, R. D. (1979). Changes in *Epilobium* phyllotaxy induced by N-1-naphthylphthalamic acid and  $\alpha$ -4-chlorophenoxyisobutyric acid. *Am. J. Bot.* **66**, 557–569.
- MEICENHEIMER, R. D. (1982). Change in *Epilobium* phyllotaxy during the reproductive transition. *Am. J. Bot.* **69**, 1108–1118.
- MEICENHEIMER, R. D. (1987). Role of the stem growth in *Linum usitatissimum* leaf trace patterns. *Am. J. Bot.* **74**, 857–867.
- MEINHARDT, H. (1974). The formation of morphogenetic gradient and fields. *Ber. Deutsch. Bot. Ges.* **87**, 101–108.
- MITCHISON, G. H. (1977). Phyllotaxis and the Fibonacci series. *Science* **196**, 270–275.
- PLANTEFOL, L. (1948). *La Théorie des Hélices Foliaires*. Paris, Masson.
- RICHARDS, F. J. (1948). The geometry of Phyllotaxis and its origin. *Soc. Exp. Biol. Symp.* **II**, 217–245.
- RICHARDS, F. J. (1951). Phyllotaxis: its quantitative expression and relation to growth in the apex. *Phil. Trans. R. Soc. Lon. B* **225**, 509–564.
- RIVIER, N. (1988). Crystallography of spiral lattices. *Mod. Phys. Lett. B* **2**, 953–960.
- ROTHEN, F. & KOCH, A. J. (1989). Phyllotaxy or the properties of the spiral lattices. (I) Shape invariance under compression. *J. Physique* **50**, 633–657 and (II) Packing of circles along logarithmic spirals. *J. Physique* **50**, 1603–1621.
- RUTISHAUSER, R. (1982). Der plastochronquotient als Teil einer quantitativen Blattselungsanalyse bei Samenpflanzen. *Beitr. biol. Pflanzen* **57**, 323–357.
- RYAN, G. W., ROUSE, J. L. & BURSILL, L. A. (1991). Quantitative analysis of sunflower seeds packing. *J. theor. Biol.* **147**, 303–328.
- SACHS, T. (1991). *Pattern Formation in Plant Tissues*. Cambridge, Cambridge University Press.
- SCHIMPER, K. F. (1830). Beschreibung des Symphytum Zeyheri und seiner zwei deutschen Verwandten der *S. Bulborum* Schimp und *S. Tuberosum*. *Jacq. Geiger's Mag. für Pharm.* **29**, 1–92.
- SCHOUTE, J. C. (1913). Beiträge zur Blattstellungslehre. *Rec. Trav. Bot. Néerl.* **10**, 153–339.
- SCHWABE, W. W. (1971). Chemical modification of phyllotaxis and its implication. *Soc. Exp. Biol. Symp.* **25**, 301–322.
- SCHWENDENER, S. (1878). *Mechanische Theorie der Blattstellungen*. Leipzig, Engelmann.
- SNOW, M. & SNOW, R. (1935). Experiments on phyllotaxis. 3. Diagonal splits through decussate apices. *Phil. Trans. R. Soc. Lon. B* **225**, 63–94.
- SNOW, M. & SNOW, R. (1952). Minimum area and leaf determination. *Proc. R. Soc. Lon. B* **139**, 545–566.
- SNOW, M. & SNOW, R. (1962). A theory of the regulation of phyllotaxis based on *Lupinus albus*. *Phil. Trans. R. Soc. Lon. B* **244**, 483–513.
- STEEVES, T. A. & SUSSEX, I. M. (1989). *Patterns in Plant Development*. Cambridge, Cambridge University Press.
- TURING, A. M. (1952). The chemical basis of morphogenesis. *Phil. Trans. R. Soc. Lon. B* **237**, 37–72.

- VAN ITERSON, G. (1907). *Mathematische und Microscopisch-Anatomische Studien über Blattstellungen, nebst Betrachtungen über den Schalebau der Miliolinen*. Iena, Gustav-FischerVerlag.
- VEEN, A. H. & LINDENMAYER, A. (1977). Diffusion mechanism for phyllotaxy. *Plant Physiol.* **60**, 127–139.
- WARDLAW, C. W. (1968). *Essays on Forms in Plants*. Manchester: Manchester University Press.
- WEISSE, A. (1897). Die Zahl der Randblüthen an Compositenköpfchen in ihrer Beziehung zur Blattstellung und Ernährung. *Jahrb. Wiss. Bot.* **30**, 453–483.
- WILLIAMS, R. F. (1975). *The Shoot Apex and the Leaf Growth*. Cambridge: Cambridge University Press.
- WILLIAMS, R. F. & BRITTAIN, E. G. (1984). A geometrical model of phyllotaxis. *Aust. J. Bot.* **32**, 43–72.
- YOUNG, D. A. (1978). On the diffusion theory of phyllotaxis. *J. theor. Biol.* **71**, 421–432.